Proceedings of ICRC 2001: 381 © Copernicus Gesellschaft 2001

ICRC 2001

Cosmic ray energy spectrum above 3×10^{17} eV measured with the Haverah Park Array

M. Ave[1], J. A. Hinton[2], J. Knapp[1], J. Lloyd-Evans[1], M. Marchesini[1], and A .A. Watson[1]

[1]Department of Physics and Astronomy, University of Leeds, Leeds LS2 9JT ,UK
[2]Enrico Fermi Institute, University of Chicago, Chicago, IL 60637, USA

Abstract. The energies of air showers recorded at the Haverah Park Array have been re-estimated using the CORSIKA program. As in the original analysis the cosmic ray energy was determined via its relation to the ground-level parameter $\rho(600)$. This relation was obtained previously through simulations with a rather simple hadronic interaction model. In this work we use CORSIKA with QGSJET to model air showers and GEANT to simulate the detailed detector response to ground particles, leading to a modified relation between $\rho(600)$ and the primary energy. A revised energy spectrum is reported for 3×10^{17}eV $< E < 4 \times 10^{18}$ eV.

1 Introduction

At Haverah Park (HP) a 12 km^2 air shower array consisting of water-Cherenkov detectors was operational from 1967-1987 to measure cosmic rays (CR) in the energy range 3×10^{17} eV to 10^{20} eV (Lawrence et al., 1991). Here we present a re-analysis of some of the data taken in the period 1974-1987. Previously the energy reconstruction was obtained using simulations by Hillas et al. (1971). A variety of more sophisticated models for hadron production have become available that are based on Gribov-Regge theory and attempt to include QCD in a consistent way. CORSIKA (Heck et al., 1998), using QGSJET (Kalmykov et al., 1997) for high energy hadronic interactions, is such a model and reproduces a variety of experimental results from 10^{12} to 10^{20} eV. Also the detector response to shower particles is simulated in much greater detail than was possible 30 years ago. In this paper we present a re-analysis of HP data using CORSIKA/QGSJET and GEANT (Brun et al., 1993), and a revised energy spectrum from an improved reconstruction algorithm.

Correspondence to: M. Ave (ave@ast.leeds.ac.uk)

2 The Haverah Park Array

The HP extensive air shower array was situated near Leeds, UK, at an altitude of 220 m asl. (atm. depth = 1016 g cm^{-2}) at 53° 58′ N, 1° 38′ W. Particles were detected with water-Cherenkov counters of approximately 2.29 m^2 area $\times 1.2$ m depth, viewed by a photomultiplier tube (PMT). The number of Cherenkov photons released in a water tank is proportional to the energy deposit of the shower particles in the water. Shower electrons and photons, with typical energies of 1-10 MeV, are effectively stopped, while muons penetrate the tank and release a number of photons that is proportional to their track length in the water. As most of the energy of an air shower at ground is carried by the electromagnetic particles this technique is very effective at measuring the energy flow in the shower disc. The densities of Cherenkov photons per unit detector area (Cherenkov densities) were recorded in terms of the average signal from a vertical muon (1 vertical equivalent muon = 1 vem) per square metre. This signal corresponds to ≈ 14 photoelectrons (pes) (Evans, 1971). Detector areas larger than 2.29 m^2 were achieved by grouping different numbers of these modules. The central triggering tanks were 34 m^2 are detectors made of 15 modules. The signals from the 15 modules were summed to provide the signal used for triggering and for the density estimate. A 16$^{\rm th}$ tank in each group was used to provide a low gain signal. Fig. 1 shows the overall layout of the Haverah Park Array. The trigger was formed if in the A1 detector and in at least 2 out of the three other A-sites (A2-A4) a density of $>$0.3 vem m^{-2} was recorded. Trigger rates were monitored daily over the lifetime of the experiment and were stable, after correction for atmospheric pressure variations, to better than 5%. The detector groups B-G are surrounding the A detectors at about 2 km distance do not usually show signals above threshold in the energy range we are interested in; however they constrain the core position inside the array. Additionally there is an internal ring of three 9 m^2 detectors at 150 m from the centre of the array. The data from 1974-1987 include for each event

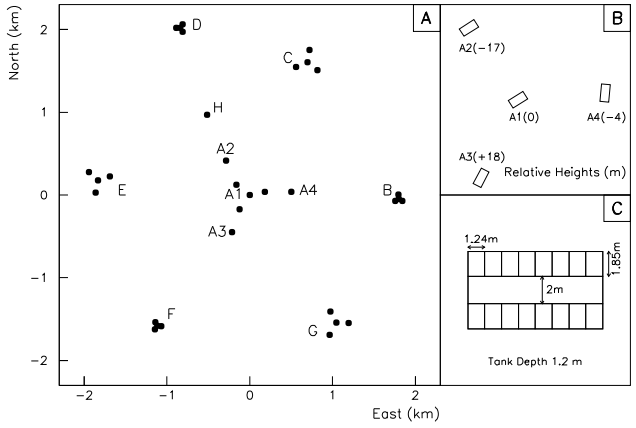

Fig. 1. Layout of the HP array. A) The whole array. B) The orientations of the detector huts A1-A4. C) The arrangement of water tanks within an A-site detector hut.

the densities and arrival times of shower particles for each detector. In a typical event the 7 central detectors have signals recorded. For each event also the reconstructed θ, ϕ, core position x,y, and $\rho(600)$ are stored from the original analysis. In total 84455 events with $0^\circ < \theta < 45^\circ$ and $E > 2 \times 10^{17}$ eV are available.

3 Arrival Direction, Core Position and Shower Size

First the direction of the CR is determined by fitting a plane to the particle arrival times recorded at the detectors A1 to A4. The error in θ as determined by comparison with a muon tracking device was $\sigma_\theta = 2.5^\circ \sec\theta$, for $0^\circ < \theta < 45^\circ$. We use the directions as determined by the original HP analysis. With θ and ϕ known, the detectors coordinates are projected into the shower plane passing through A1. Then the core location x,y and the Cherenkov density at 600 m from the shower core, $\rho(600)$, are found by assuming a shape of the lateral distribution function (LDF) and performing a fit of the LDF to the measured densities. The LDF of the water-Cherenkov signal $\rho(r)$, in units of vem m^{-2}, is well described for r = 50-800 m by $\rho(r) = k\ r^{-(\eta + r/4000\ \mathrm{m})} = k\ f(r)$, where k is a normalization constant, and η is given by $\eta = 3.78 - 1.44\ \sec\theta$. With the small number of densities in a normal event, it is not possible to fit reliably values of η for individual showers. The function $\eta(\theta)$ was calculated from average water-Cherenkov LDFs for different θ bins and is in good agreement with simulation results. For a given core position and θ we assume an LDF (initially with η fixed to its mean value for the given θ) and calculate the shower size constant k. We use only detectors with densities above threshold and below the saturation density. The variances σ_i^2 to enter the fit are obtained by adding in quadrature all sources of errors: $\sigma_i^2 = \rho_i^2\ (\sigma(\rho)/\rho)^2 + X_i^2 + \rho_i/(p_i\ A_i) + \rho_i/(15\ A_i)$, where the first term is the absolute measurement error, X_i is a constant error in ρ due to digitisation, and the other terms are Poisson errors in the number of particles and Cherenkov photons, respectively. p_i is a factor which is the effective number of particles that make up the signal of a vertical equivalent muon. Its value was determined from the parameterization of $\mu/C(\theta, r)$ in Shelley (1982), which is the fraction of Cherenkov signal, $C(\theta, r)$, released by the muons . This procedure allows us to compute a likelihood function which is maximised by varying k, x, y, and η in a gradient search. The value of $\rho(600)$ is then obtained from k and the corresponding value of η. The main differences between this analysis and the original HP algorithm are that the parameter η is variable in the fit and p_i is changing with θ and core distance, while it was assumed to be constant originally. Over 8000 events were re-analysed. Requiring the core position to be < 300 m away from A1 and $\theta < 45^\circ$ ensures 100 % trigger efficiency for $E > 4 \times 10^{17}$ eV, allowing a simple calculation of the effective area needed for the reconstruction of the energy spectrum.

4 Calibration via Simulated Events

Detector Response: A detailed GEANT simulation of electrons, gammas, and muons under different zenith and azimuth angles in HP detectors has been performed. Cherenkov photons were ray-traced until they were absorbed or fall on the photocathode of the PMT. The wavelength dependence of light absorption in the water, wall reflectivity and PMT quantum efficiency have been taken into account. At a typical energy of 1 GeV a vertical muon yields about 14 pes in a HP tank, in good agreement with experimental results (Evans, 1971). The mean energy of e and γ in vertical showers is < 10 MeV. Convolving the energy spectra with the detector response, mean signals of 2.6 and 0.9 pes are obtained for vertical e and γ, respectively. The mean e/γ signals vary by less than 15% for $0^\circ < \theta < 45^\circ$. The muon signal varies with its track length in the water, i.e. with θ, but this is compensated partially by the change of the effective (projected) area the detector presents to incoming particles. The mean signals from μ, e, and γ at different energies and zenith angles are used to produce the water-Cherenkov LDF for individual events from Monte Carlo simulations. The use of mean values, instead of the sampling the signal distribution, was shown to have no noticeable effect on the resulting LDF.

Air Shower Simulations: Simulations with CORSIKA 6.0 were used to obtain primary energies from the measurements. High energy hadronic interactions were modeled with QGSJET. In total 3600 showers of primary protons and iron were simulated with $0^\circ < \theta < 45^\circ$ and 2×10^{17} eV $< E < 6.4 \times 10^{18}$ eV. Statistical thinning of shower particles was applied at the level of $10^{-6} \times E_0$ with a maximum particle weight limit of $10^{-13} \times E_0$/eV. For each set of simulation parameters 100 showers have been simulated. The CORSIKA output was convolved with the tank response and the resulting LDF was fitted for each individual shower. To increase the statistics each shower was thrown 100 times onto the array with random core positions ranging out to 400 m from the centre of the array. The zenith angles for these multiple

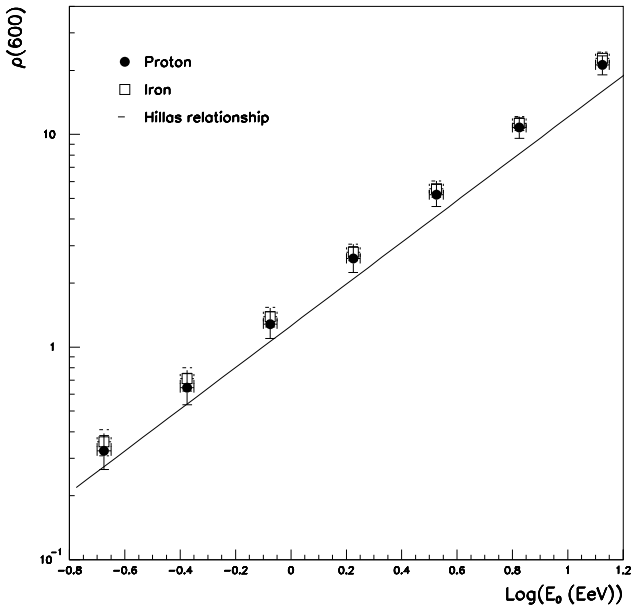

Fig. 2. $\rho(600)$ as function of E_0 for proton and iron showers at $\theta = 26^\circ$, from CORSIKA/QGSJET simulations. Simulation results by Hillas et al. (1971) are plotted as solid line.

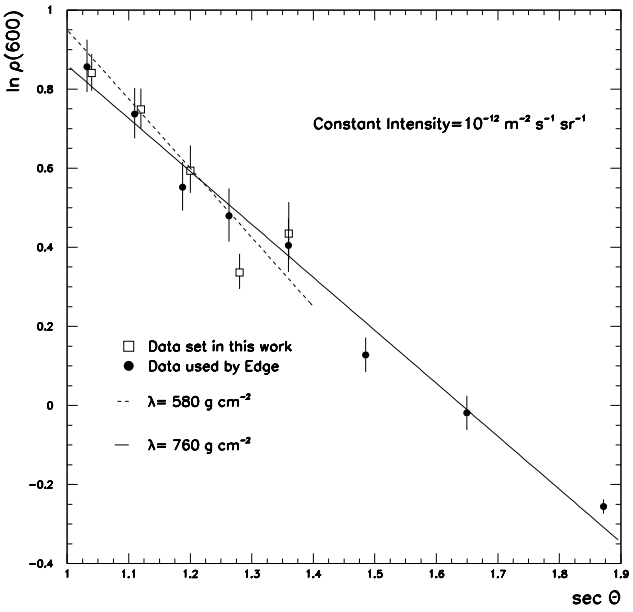

Fig. 3. Attenuation of $\rho(600)$ with zenith angle deduced with the constant intensity cut method. Results by Edge et al. (1973) are compared with our analysis.

Monte Carlo events is obtained fluctuating θ of their parent event with the angle measurement error. The particle densities are modified according to Poisson fluctuations in the number of particles. If an event fulfills the array trigger conditions the densities are fluctuated according to measurement errors and recorded in the same format as real data. Each simulated event is analysed like real data to find its core position and $\rho(600)$.

Energy Calibration: The primary energy of a shower is determined from the measured $\rho(600)$. We have studied $\rho(600)$ at $\theta = 26^\circ$ since the majority of the showers in the data arrived at around this angle. The calibration curves for p an Fe primaries are plotted in Fig. 2, and are compared with simulation results from Hillas et al. (1971), that were used for previous HP analyses. $\rho(600)$ grows linearly with E_0, demonstrating again that $\rho(600)$ is a good energy indicator. The values of $\rho(600)$ for iron showers are $\approx 10\%$ higher than those for proton showers, almost independent of energy. The energy calibration is parameterised by $E_0(\mathrm{in\ EeV}) = 0.612 \times \rho(600)^{0.99}$ for p and $E_0(\mathrm{in\ EeV}) = 0.567 \times \rho(600)^{1.00}$ for Fe, with an uncertainty in the constants and slopes of about 1% for p and 0.5% for Fe. There is a noticeable difference between the *old* and the *new* calibration, which leads to at least $\approx 30\%$ lower reconstructed energies at about 10^{18} eV.

Attenuation Length: Showers of different zenith angles are combined to derive an energy spectrum. The observed density $\rho(\theta, r)$ at zenith angle θ and core distance r is corrected to that at 26° using the relation:

$$\rho(r, \theta = 26^\circ) = \rho(r, \theta) \exp\left(\frac{X_{\mathrm{obs}}}{\lambda}(\sec\theta - \sec 26^\circ)\right)$$

where X_{obs} is the atmospheric depth of the observation level and λ is the attenuation length of $\rho(600)$. λ can be measured with the constant-intensity-cut method. Fig. 3 summarises the results from this method on HP data as obtained by Edge et al. (1973). Using a cut at 10^{-12} m^{-2} s^{-1} sr^{-1} for $0^\circ < \theta < 60^\circ$ a value of $\lambda = 760 \pm 40$ g cm^{-2} was found by a linear least-square fit giving all points equal weight. We have repeated the analysis on a different data set (1974-1987), but restricted to zenith angles $\theta < 45^\circ$ and with the individual errors of each point. Our data points are compatible with the previous ones at for $\theta < 45^\circ$, but our value of λ is 580 ± 50 g cm^{-2}. The disagreement comes from the different θ range used and is qualitatively understandable. The attenuation of $\rho(600)$ with θ is a result of the attenuation of the electromagnetic and muonic components. The muonic component attenuates slower, so when its contribution to $\rho(600)$ dominates the λ will increase. The present analysis is restricted to $\theta < 45^\circ$. The experimental value fits well, within the errors, to the simulations for p (512 g cm^{-2}) and Fe showers (580 g cm^{-2}).

Energy Resolution: The energy resolution has a direct impact on the reconstruction of a steep spectrum. Finite resolution shifts and varying resolution tilts the spectrum. The energy resolution, a combination of measurement errors and fluctuations, was determined from simulations as function of mass, E and θ. For p shower and a realistic mix of zenith angles $\sigma(E)/E = 17\%$ at 0.4 EeV and 12% at 6.4 EeV were obtained. Fe showers had $\approx 30\%$ better resolution due to smaller intrinsic fluctuations. The effect of the energy resolution on the intensities in the final energy spectrum is less than 2%, so no correction was performed.

Core Position: According to simulations the core position can be determined with a precision of ≈ 15 m.

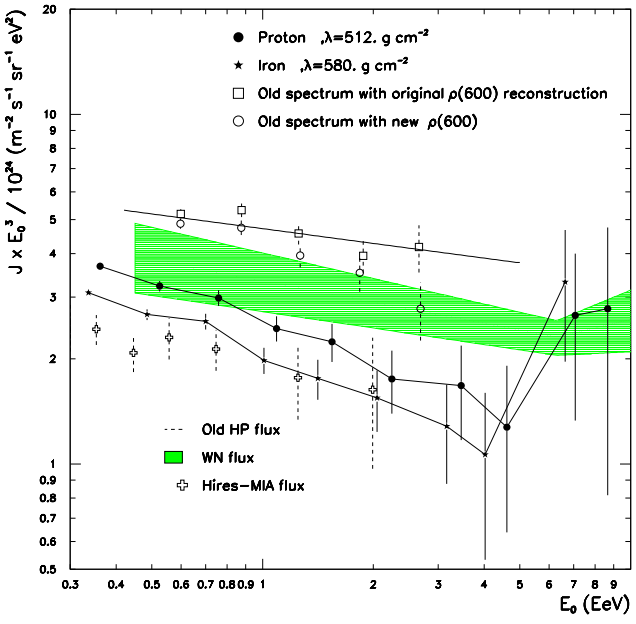

Fig. 4. Energy spectrum obtained from HP data compared with other spectra. The shaded area give the flux as compiled by Nagano and Watson (2000).

5 Energy Spectrum

The energy spectrum was deduced from showers with cores located within 300 m of the array centre and $\theta < 45°$. We also required $\rho(600, 26°) > 0.5$ vem m^{-2} to ensured a 100% trigger efficiency for all events, independent of LDF, within the 300 m radius. The total on-time for these events was 3.657×10^8 seconds, about 11 years. The total effective exposure is 7.39×10^{12} m^2 s sr. 3500 events survive all selection cuts. This number varies up to 2% when varying λ within its uncertainty, and increases by 30% when the old HP value of $\lambda = 760$ g cm^{-2} is used. Fig. 4 shows the differential energy spectra assuming proton or iron primaries, respectively. Also spectra from other experiments (Abu-Zayyad, 2001) and from a recent compilation of experimental results (Nagano and Watson, 2000) are shown. Two sets of points are drawn for the *old* HP flux, corresponding to the cases in which the *old* λ (760 g cm^{-2}) and the Hillas E-$\rho(600)$ relation were retained but the reconstructed $\rho(600)$ was taken from the original analysis or from the improved algorithm. There is a distinct difference between them which can be attributed to a bias in the original analysis, such as non-Gaussian energy resolution. The difference in the normalization between the *old* HP spectrum and the one presented here is consistent with the 30% difference in the E-$\rho(600)$ relation convolved with the steep energy spectrum. A least-square fit to the experimental fluxes in the range 3×10^{17} eV$< E < 4 \times 10^{18}$ eV is consistent with a power law of the form $dN/dE = J \times 10^{-30}\mathrm{m}^{-2}\,\mathrm{s}^{-1}\,\mathrm{sr}^{-1}\,\mathrm{eV}^{-1} \times (E_0/10^{18}\mathrm{eV})^{\gamma}$ with $J = 2.03 \pm 0.07$ and $\gamma = -3.36 \pm 0.04$ for p showers and with $J = 2.55 \pm 0.09$ and $\gamma = -3.38 \pm 0.04$, assuming Fe showers.

6 Highest Energy Events

Using the new $\rho(600)$-E relation, and assuming proton primaries and $\lambda = 540$ g cm^{-2}, the energies of the 4 largest events (Lawrence et al., 1991) have been recalculated. The energies are reduced by about 30%. The new and smaller λ to some extent compensates for the lower $\rho(600)$ to energy conversion factor. The largest event is now estimated to have an energy of 8.28×10^{19} eV.

7 Conclusions

The energy spectrum obtained in this analysis shows differences of up 30% with a recent spectrum derived from Akeno and Haverah Park data (Nagano and Watson, 2000). Our results are compatible with the new results of the HIRes-Mia experiment for pure iron composition (Abu-Zayyad, 2001). Since the spectral index just above the *knee* is between 3.11 and 3.25 (Antoni et al., 2001), a break in the primary energy spectrum between the 6×10^{15} eV and 3×10^{17} eV is needed to connect to our value. The break at $\approx 3 \times 10^{17}$ eV, as claimed by Abu-Zayyad (2001), is unfortunately right at the low-energy end of the range considered in this analysis. This work will be extended to higher energies, but the procedure to obtain the spectrum above the *ankle* has to be rather different from what was presented here. The strict 300 m cut cannot be used and algorithms to reconstruct the shower parameters need modification. Further analysis is in progress. The Haverah Park array can be considered as an early prototype of the array of the Auger Observatory which will employ water-Cherenkov tanks of identical depth. The steps towards an energy spectrum from the Auger array are very similar to those described here, and similar problems, such as the choice of the appropriate attenuation length and the $\rho(r)$-E relation, need to be solved in the near future.

Acknowledgements. Thanks are given to members of the Haverah park group who helped to get the data discussed here over 20 years ago. In particular the major contributions made by Dr R J O Reid are gratefully acknowledged. We also acknowledge the support of the computing centre of IN2P3 in Lyon, where the simulations were performed.

References

Abu-Zayyad T. et al., Ap. J. (to be published), astro-ph/0010652.
Antoni T. et al., Astrop. Phys. (2001) in press
Brun R. et al., GEANT, Detector Description and Simulation Tool, CERN, Program Library CERN (1993).
Edge D.M. et al., J. Phys A **6** (1973) 1612
Evans A., PhD Thesis (1971), University of Leeds.
Heck D. et al., FZKA 6019, Forschungszentrum Karlsruhe, 1998.
Hillas A.M. et al., Proc. 12$^{\mathrm{th}}$ Int. Cosmic Ray Conf., Hobart **3** (1971) 1001
Kalmykov N. et al., Nucl. Phys. B 52B (1997) 17
Lawrence M.A. et al., J. Phys. G **17** (1991) 733
Nagano M., Watson A.A., Rev. Mod. Phys. **72** (2000) 689 and refs. therein.
Shelley C.C., PhD Thesis (1982), University of Nottingham